Department of Physics and Astronomy
University of Heidelberg

Bachelor Thesis in Physics
submitted by

Jan Sören Breidenbach

born in Frankfurt am Main-Höchst (Germany)

2018

Hadronic vacuum polarization in atoms

This Bachelor Thesis has been carried out by Jan Sören Breidenbach at the
Max Planck Institute for Nuclear Physics in Heidelberg
under the supervision of
PD Dr. Zoltán Harman

Abstract

In this Bachelor thesis the energy shift in atoms due to hadronic vacuum polarization is evaluated. A hadronic polarization function for the photon propagator is obtained from experimental $e^-/e^+ \to$ hadronic matter-collision data via the optical theorem and the Kramers-Kronig relations. An effective central potential is calculated applying a parameterization for this polarization function. The energy corrections to a Coulomb potential originating from hadronic vacuum polarization are calculated using the analytical bound Dirac-Coulomb wave functions, as well as relativistic bound wave functions considering the finite nuclear size. These results are compared to results from a non-relativistic theory.

In dieser Bachelorarbeit wird die Energieverschiebung in Atomen aufgrund von hadronischer Vakuumpolarisation berechnet. Eine hadronische Polarisationsfunktion des Photonenpropagator wird aus experimentellen $e^-/e^+ \to$ hadronischer Materie-Kollisionsdaten mithilfe der Kramers-Kronig Relationen und des optisches Theorems erstellt. Ein effektives Zentralpotential wird aus einer Parametrisierung der Polarisationsfunktion bestimmt. Die Energieverschiebung durch die hadronische Vakuumpolarisation im Vergleich zu einem Coulumbpotential wird mithilfe der analytischen gebundenen Dirac-Coulomb Wellenfunktionen, sowie mit relativistischen gebundenen Wellenfunktionen für ausgedehnte Atomkerne, berechnet. Diese Ergebnisse werden mit den Ergebnissen einer nicht relativistischen Theorie verglichen.

Contents

1 Introduction

In this thesis we investigate the correction to the energy of a lepton in hydrogen-like ions due to virtual hadronic pair creation. Quantum electrodynamics (QED) has been well tested in the case of weak fields, therefore the current research is rather interested in the QED of strong external fields and in explaining more details of the interaction process itself. Highly charged hydrogen- or lithium-like ions provide possibilities to analyze and test these strong-field effects because only few electrons are exposed to a very strong field. Thereby effects other than the pure interaction between the nucleus and the electron are minimized. Quantities such as the fine structure splitting or the g-factor can nowadays be measured and evaluated theoretically with high accuracy [1]. Combining these theoretical estimates with spectroscopic high-precision measurements also enables to improve the accuracy of fundamental constants. An example is the determination of the electron mass from the g-factor measurement of H-like carbon ions [2], which yielded an exceeding one order of magnitude more accurate result compared to the previous CODATA value. In the future, the value for the fine-structure constant could also be improved with measurements of heavy ions, such as lead [3], demanding a very precise theoretical description. One of the key ideas is to minimize the restricting uncertainty from nuclear effects by a weighted difference of the g factors of an H- and a Li-like ion from the same element.

This thesis concentrates on the vacuum polarization (VP) correction whose biggest contribution arises from virtual e^+/e^- pair creation. This contribution is well understood and will only be discussed here due to its importance and as reference for further corrections. The next important contribution is μ^+/μ^- pair creation, which is suppressed in its effect because the muon is about 207 times heavier than the electron. Apart from the mass, the muonic-loop description is equivalent to that of the electronic case, although this effect is much more sensitive to nuclear corrections. After this, the next contributions stem from several different hadronic particles, which ask for a completely different description since they also interact via the strong interaction. The quantum field theory to describe strongly interacting particles, quantum chromodynamics (QCD),

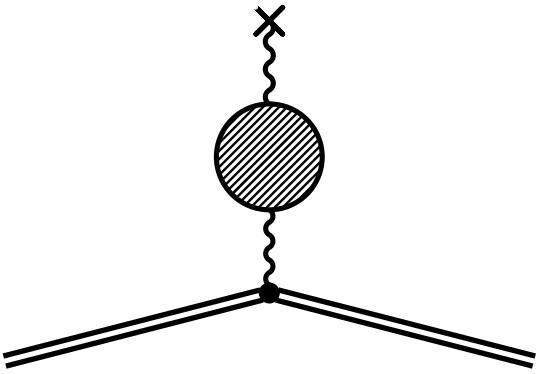

Figure 1.1: Feynman diagram depicting the hadronic vacuum polarization effect. The double lines represent a bound electron that interacts with the Coulomb field of a nucleus (the wave line terminated by a cross) via a photon that is modified by hadronic vacuum polarization represented by the shaded loop.

can be approached perturbatively only for large energies. The low-energy section yields the most important contribution for the hadronic VP energy shift, therefore, it has to be dealt with in another way. We describe how the VP can be characterized by the total hadronic cross section. First descriptions used contributions of single hadronic particles, such as the ρ-meson [4], one of the most important contributions to the hadronic VP. In this thesis a semi-empirical approach will be employed to deal with the whole hadronic contribution at once. An effective potential can be constructed from a parameterized hadronic VP function. Then energy shifts can be calculated, using different approaches: a analytical non-relativistic approximation for a point-like nucleus, the Uehling potential from an extended homogeneous charged nucleus as a 1^{st}-order perturbation to the analytical Dirac-Coulomb wave functions and as a 1^{st}-order perturbation to the Coulomb wave functions of an extended nucleus, and finally with the exact wave functions from the Uehling potential from an extended homogeneously charged nucleus and thereby, for all orders. These calculations will be done for the hydrogen-like systems H, Si, Ca, and Pb, and additionally for muonic hydrogen. The results for the different approaches will then be discussed in their uncertainty and applicability.

All the formulas in this thesis are given in natural units, where the speed of light and the reduced Planck constant are set to one. Furthermore the Einstein summation convention and the Feynman slash notation are used, such as:

$$\vec{\gamma}\cdot\vec{p} = \sum_{i=1}^{3}\gamma^i p^i = \gamma^1 p^1 + \gamma^2 p^2 + \gamma^3 p^3\,,$$
$$\not{p} = \gamma^\mu p_\mu = \sum_{i=0}^{3}\gamma^i p_i = \gamma^0 p^0 - \gamma^1 p^1 - \gamma^2 p^2 - \gamma^3 p^3\,. \tag{1.1}$$

The anti-commutator of two operators a and b is given by

$$\{a, b\} = ab + ba\,. \tag{1.2}$$

2 Vacuum polarization

In the case of strong fields or when precise theoretical predictions are needed one has to consider several effects in quantum field theory. For quantum electrodynamics (QED), the appearing contributions can be classified into three categories: self-energy corrections, vertex corrections and virtual e^+/e^- pair creation.

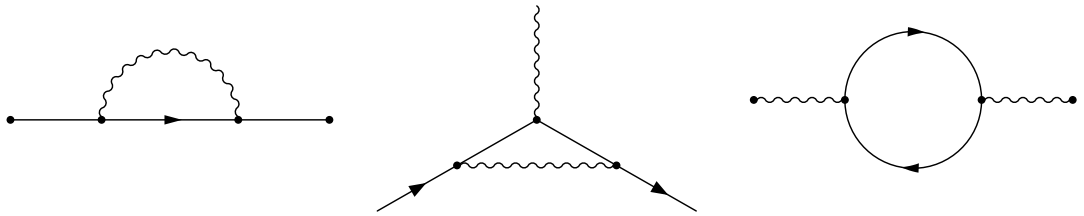

(a) Self-energy correction (b) Vertex correction (c) Virtual e^+/e^--pair production

Figure 2.1: QED loop corrections: A straight line denotes a free electron propagator, and a wave line denotes a photon.

2.1 Modification of the photon propagator

This thesis focuses on the latter contribution, which is often called vacuum polarization (VP). It describes the modification of the Feynman photon propagator which is given in unperturbed form in Feynman gauge as

$$iD_{\mu\nu}(q) = \frac{-i4\pi\eta_{\mu\nu}}{q^2 + i\epsilon}\,. \tag{2.1}$$

with the momentum q, the Minkowski metric tensor $\eta_{\mu\nu} = \mathrm{diag}\,(1, -1, -1, -1)$, and ϵ representing an arbitrarily small positive real number to ensure causal time ordering in the Feynman propagator. The first QED correction to the photon propagator $D'_{\mu\nu}$ is of

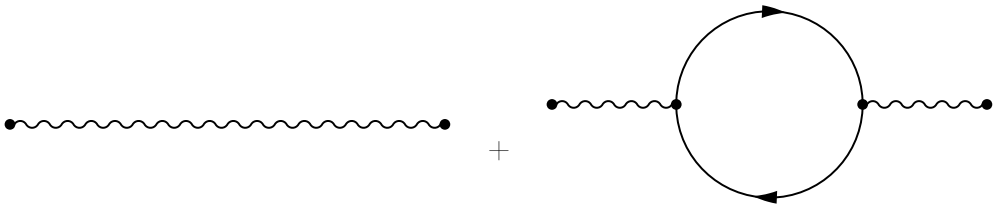

(a) Unmodified photon propagator

(b) 1st-order in α photon propagator correction

Figure 2.2: Photon propagator correction due to VP represented by a Feynman diagram.

order $e^2 \equiv \alpha$, with the elementary charge e and the fine-structure constant α. Using the Feynman rules of QED [5], the modified propagator can be written as

$$iD^{\mathrm{mod}}_{\mu\nu}(q) = iD_{\mu\nu}(q) + iD_{\mu\lambda}\frac{i\Pi^{\lambda\sigma}(q)}{4\pi}D_{\sigma\nu}\,, \tag{2.2}$$

with the VP tensor $\Pi_{\mu\nu}(q)$ given by

$$\Pi_{\mu\nu}(q) = 4\pi i\alpha \int \frac{d^4k}{(2\pi)^4}\frac{\mathrm{Tr}(\gamma_\mu(\not{k}+m\mathbb{1})\gamma_\nu(\not{k}-\not{q}+m\mathbb{1}))}{(k^2-m^2+i\epsilon)((k-q)^2-m^2+i\epsilon)}\,. \tag{2.3}$$

with the lepton mass m and the integration over the momentum k of one of the loop particles. The trace originates from the cyclicity of the spinor indices and an additional factor of (-1) has to be included because of the closed fermionic loop. One can evaluate this further using γ-trace identities:

$$\begin{aligned}\Pi_{\mu\nu}(q) &= 16\pi i\alpha \int \frac{d^4k}{(2\pi)^4}\frac{k_\mu(k-q)_\nu + (k-q)_\mu k_\nu - \eta_{\mu\nu}(k^2 - q\cdot k - m^2)}{(k^2-m^2+i\epsilon)((k-q)^2-m^2+i\epsilon)} \\ &\equiv \int d^4k\, h_{\mu\nu}\left(q,k,m^2\right)\,. \end{aligned} \tag{2.4}$$

This integral diverges quadratically but it can be regularized, for example by the Pauli-Villars regularization scheme [6]. This regularization method isolates finite parts from diverging ones and provides counterterms for the diverging terms. The counterterms can

be thought of as originating from fictitious particles with masses M_i. The regularized polarization tensor reads

$$\bar{\Pi}_{\mu\nu}(q) = \int d^4k \Bigg(h_{\mu\nu}\left(q, k, m^2\right) + \sum_{n=1}^{N} C_i f_{\mu\nu}\left(q, k, M_i^2\right) \Bigg) . \tag{2.5}$$

The fictitious masses M_i and associated constants C_i are chosen in a way that the regularized polarization tensor is convergent. The evaluation of the integral is not trivial, and can be followed in detail for example in [5]. In the end it is apparent that physical observables are independent of these arbitrarily introduced parameters. The final result for the regularized polarization tensor $\bar{\Pi}_{\lambda\sigma(q)}$ is

$$\bar{\Pi}_{\lambda\sigma}(q) = (q^2\eta_{\lambda\sigma} - q_\lambda q_\sigma)\bar{\Pi}(q^2) = (q^2\eta_{\lambda\sigma} - q_\lambda q_\sigma)\left[\frac{-\alpha}{3\pi}\ln\frac{\Lambda^2}{m^2} + \Pi^{\mathrm{R}}(q^2)\right], \tag{2.6}$$

with the polarization function $\bar{\Pi}(q^2)$, a cut-off momentum Λ and the regular part of the polarization function given by

$$\Pi^{\mathrm{R}}(q^2) = \frac{2\alpha}{\pi}\int_0^1 d\beta\beta(1-\beta)\ln\left[1 - \beta(1-\beta)\frac{q^2}{m^2}\right]. \tag{2.7}$$

The logarithmically divergent part is included in the definiton of the measurable elementary charge [6]. From now on, only the regular part of the polarization function will be evaluated and the charge is assumed to be the measurable renormalized charge.

2.2 The Uehling potential

In order to describe the effect of VP for bound systems like atoms, the potential of the nucleus can be written as a convolution of the modified photon propagator $D'_{\mu\nu}(x)$ with the current $j_\mu(x)$. The VP is thereby described by an effective potential, called the Uehling potential. In momentum space it can be written as a simple multiplication:

$$A_\mu^{\mathrm{mod}}(x) = \int \frac{d^4q}{(2\pi)^4} e^{-iq\cdot x} D_{\mu\nu}^{\mathrm{mod}}(q) j^\nu(q)\,, \tag{2.8}$$

with the modified photon propagator

$$D_{\mu\nu}^{\mathrm{mod}}(q) = \frac{-4\pi\eta_{\mu\nu}}{q^2} + \frac{-4\pi}{q^2}\left(\eta_{\mu\nu} - \frac{q_\mu q_\nu}{q^2}\right)\Pi^{\mathrm{R}}\left(q^2\right) . \tag{2.9}$$

The term with $q_\mu q_\nu$ drops out, because the continuity equation in momentum space states $q_\nu j^\nu = 0$ and the term is multiplied to such a current in Eq. (2.8). In this thesis the nucleus is approximated to be infinitely heavy compared to the electron, i.e. recoil effects get neglected, and the stationary current in position- and momentum space can be written as

$$\begin{aligned} j_\nu(x) &= j_\nu(\vec{x}) = -Ze\rho(\vec{x})\delta_{\nu 0}\,, \\ j_\nu(q) &= -2\pi Ze\,\delta(q_0)\tilde{\rho}(\vec{q})\delta_{\nu 0}\,, \end{aligned} \tag{2.10}$$

with the charge number Z and the nuclear charge density $\rho(\vec{x})$. Therefore, the nuclear Coulomb potential modified by the Uehling potential can be written as

$$A_\mu^{\mathrm{mod}}(\vec{x}) = -\,Ze\int \frac{d^3q}{(2\pi)^3}\, e^{i\vec{q}\cdot\vec{x}}\, D_{\mu 0}\left(0,\vec{q}\right)\, \tilde{\rho}\left(\vec{q}\right)\, \left[1 + \Pi^{\mathrm{R}}\left(-\vec{q}^{\,2}\right)\right]$$

$$\Leftrightarrow A_0^{\mathrm{mod}}(\vec{x}) = -\,Ze\int \frac{d^3q}{(2\pi)^3}\, e^{i\vec{q}\cdot\vec{x}}\, \frac{4\pi}{\vec{q}^{\,2}}\, \tilde{\rho}\left(\vec{q}\right)\, \left[1 + \Pi^{\mathrm{R}}\left(-\vec{q}^{\,2}\right)\right]. \tag{2.11}$$

The modified potential for leptonic VP in the case of a point-like nucleus, which is given by $\tilde{\rho}(\vec{q}) = 1$, can be rewritten further as described in [5]. The result is

$$\begin{aligned} A_0^{\mathrm{mod}}(r) &= \frac{-Ze}{r}\left[1 + \frac{2\alpha}{3\pi}\int_1^\infty d\zeta\left(1 + \frac{1}{2\zeta^2}\right)\frac{\sqrt{\zeta^2-1}}{\zeta^2}e^{-2m\zeta r}\right] \\ &= A_0^{\mathrm{Coulomb}}(r) + A_0^{\mathrm{VP}}(r)\,, \end{aligned} \tag{2.12}$$

with $r \equiv |\vec{x}|$. The modified potential is the usual Coulomb potential $A_0^{\mathrm{Coulomb}}(r)$ plus

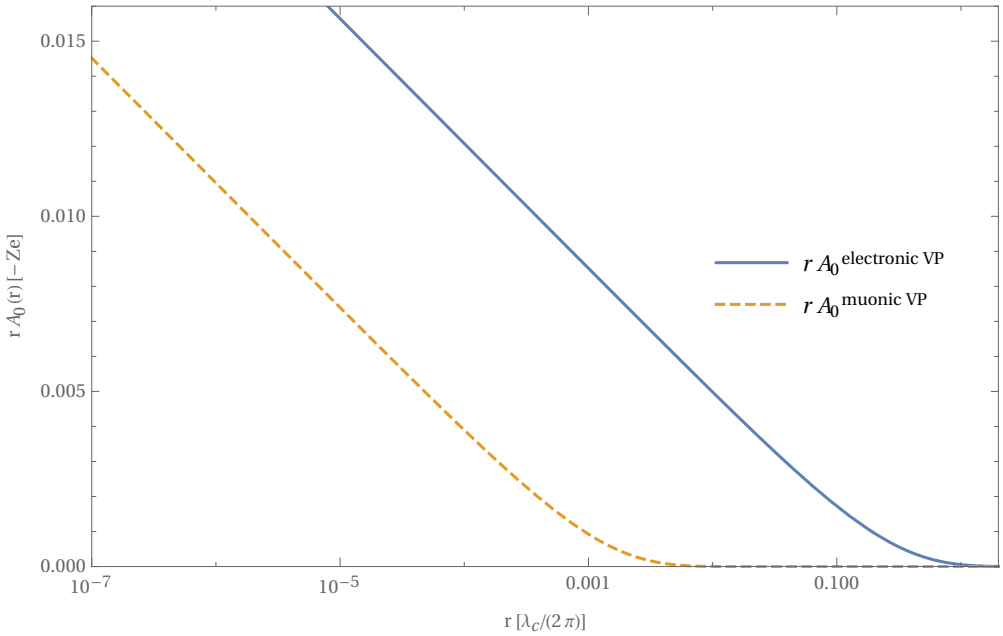

Figure 2.3: Uehling potential A_0 induced by electronic and muonic vacuum polarization divided by the Coulomb potential plotted against the radius r in units of the reduced Compton wavelength of the electron $\lambda_C/(2\pi) = 1/m_e$.

the VP contribution $A_0^{\mathrm{VP}}(r)$. From now on, only the potential $A_0^{\mathrm{VP}}(r)$ will be evaluated, although also taking into account the finite nucleus size.

The extent of the Uehling potential is approximately given by the reduced Compton wavelength $\lambda/(2\pi) = m^{-1}$ of the loop particle. Therefore, the muonic Uehling potential rises at a radius about 207 times smaller than the electronic one due to the same proportion of their masses, as shown in figure (2.3).

3 Different approaches to the vacuum polarization function

In this chapter an explicit function for the leptonic VP will be shown, as well as an approach on how to construct a VP function from another principle.

3.1 Explicit leptonic polarization function

The VP function with a virtual lepton l^+/l^--pair from Eq. (2.7) can be rewritten such that the logarithm is eliminated by partial integration. Substituting $v = 2\beta - 1$, the integral reads [5]

$$\Pi^{\mathrm{R}}(q^2) = -\frac{\alpha}{\pi}\int_0^1 dv \frac{v^2\left(1-\frac{1}{3}v^2\right)}{v^2+\frac{4m^2}{q^2}-1}\,. \tag{3.1}$$

Solving this integral is explained in detail for example in [5], here we only show the approach and the result. Integrals of this form can be related to an integral without a variable in the numerator:

$$I_n - cI_{n-2} = \int_0^1 dv \frac{v^n}{v^2-c-i\epsilon} - c\int_0^1 dv \frac{v^{n-2}}{v^2-c-i\epsilon} = \int_0^1 dv v^{n-2} = \frac{1}{n-1}\,, \tag{3.2}$$

with $c = 1 - \frac{4m^2}{q^2}$. Therefore, only a solution for I_0 is needed, which can be solved piecewise for three restricted domains. The integral has a pole at $v = \sqrt{c}$, this part will be evaluated with the residuum of the pole in addition to the principal value integral of the corresponding domain. Now the expression for the polarization function can be written as

$$\Pi^{\mathrm{R}}(q^2) = \frac{\alpha}{\pi}\left[-\frac{5}{9} - \frac{4m^2}{3q^2} + \frac{1}{3}\left(1+\frac{2m^2}{q^2}\right)d(q^2)\right], \tag{3.3}$$

$$\text{with } d(q^2) = \begin{cases} \sqrt{1-\frac{4m^2}{q^2}}\,\ln\frac{\sqrt{1-\frac{4m^2}{q^2}}+1}{\sqrt{1-\frac{4m^2}{q^2}}-1}, & \text{for } q^2 < 0\,, \\ 2\sqrt{\frac{4m^2}{q^2}-1}\,\arctan\frac{1}{\sqrt{\frac{4m^2}{q^2}-1}}, & \text{for } 0 < q^2 \leq 4m^2\,, \\ \sqrt{1-\frac{4m^2}{q^2}}\,\ln\frac{1+\sqrt{1-\frac{4m^2}{q^2}}}{1-\sqrt{1-\frac{4m^2}{q^2}}} - i\pi\sqrt{1-\frac{4m^2}{q^2}}, & \text{for } 4m^2 < q^2\,. \end{cases}$$

For squared momenta exceeding $4m^2$, the polarization function obtains an imaginary part as illustrated in figure (3.1). This can be physically explained by $2m$ being the threshold energy for particle-antiparticle production.

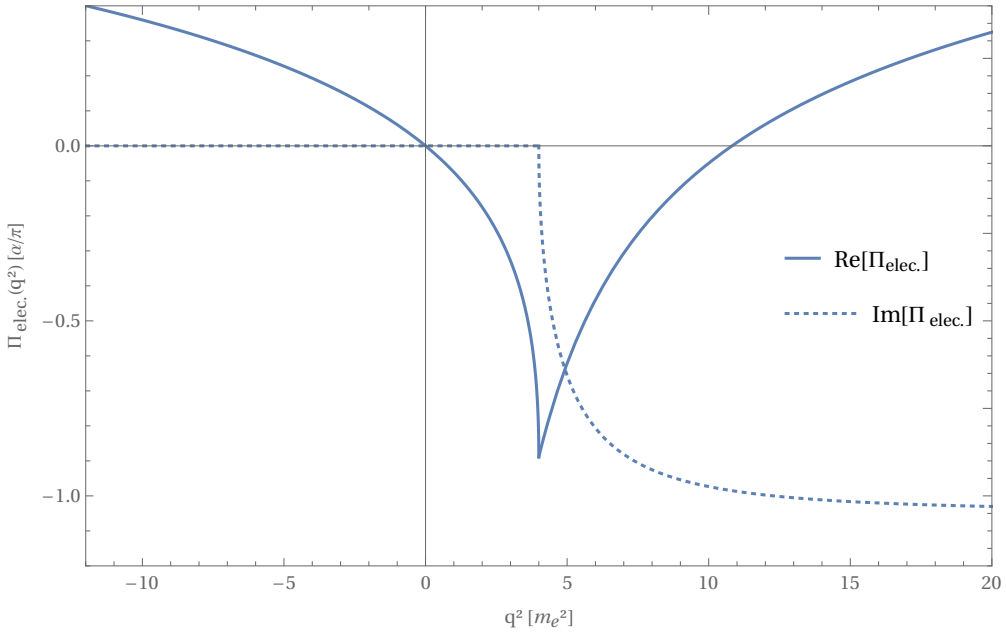

Figure 3.1: VP function for virtual e^+/e^--pair-creation plotted against the square of the momentum q in units of the electron mass m_e.

3.2 Kramers-Kronig relations

At first used in optics, the Kramers-Kronig relations describe the real part of a complex polarization function $H(x)$ in terms of its imaginary part and vice versa. They can be derived by Cauchy's integral formula and in general can be written as

$$\mathrm{Re}\left[H\left(x\right)\right] = \frac{1}{\pi} P \int_{-\infty}^{+\infty} \frac{\mathrm{Im}\left[H\left(x'\right)\right]}{x' - x} dx' \,, \tag{3.4}$$

with $P\int_a^b dx$ being the principal value integral. For our VP function the relation looks like this [10]:

$$\mathrm{Re}\left[\Pi^{\mathrm{R}}\left(q^2\right)\right] = \frac{q^2}{\pi} P \int_{-\infty}^{+\infty} \frac{\mathrm{Im}\left[\Pi^{\mathrm{R}}\left(q'^2\right)\right]}{q'^2(q'^2 - q^2 - i\epsilon)} dq'^2 \,. \tag{3.5}$$

This can explicitly be verified by inserting the imaginary part of the polarization function from Eq. (3.3):

$$\mathrm{Im}[\Pi^{\mathrm{R}}(q^2)] = \frac{\alpha}{3}\left(1 + \frac{2m^2}{q^2}\right)\sqrt{1 - \frac{4m^2}{q^2}}\,\Theta(q'^2 - 4m^2) \,, \tag{3.6}$$

with $\Theta(x)$ being the Heaviside step function. The transformation $q'^2 = \frac{4m^2}{1-v^2}$ reproduces the integral formula from Eq. (3.1).

3.3 Optical theorem

So far, the polarization function was completely determined by the fine-structure constant and the mass of the produced particles. For the electron and muon this is sufficient and their contribution has the greatest impact on VP. However, for the hadronic VP contribution one has to consider that the created particles are strongly interacting. Quantum chromodynamics (QCD) can be treated perturbatively only for large energies, furthermore, one has to take into account quite a few different hadrons that can be virtually produced. Another approach is possible due to the optical theorem, which links a measurable total cross section σ_{tot} to the forward scattering amplitude $f(k;0)$. The optical theorem reads

$$\sigma_{\text{tot}}(k) = \frac{4\pi}{|k|}\text{Im}[f(k;0)]\,, \tag{3.7}$$

with the wavenumber k. This property is a consequence of the scattering matrix S being unitary ($SS^\dagger = \mathbb{1}$). The theorem can be shown by deconstructing S into a trivial part $\mathbb{1}$, and an interaction part iT:

$$\begin{aligned} \mathbb{1} = SS^\dagger &= (\mathbb{1} + iT)(\mathbb{1} - iT)\,, \\ &= \mathbb{1} + iT - iT^\dagger + TT^\dagger\,, \\ \Leftrightarrow TT^\dagger &= i(T^\dagger - T)\,. \end{aligned} \tag{3.8}$$

The implications of the theorem are better visible when wedged between an initial and a final state:

$$\begin{aligned} \langle\psi_f|\, TT^\dagger\, |\psi_i\rangle &= i\,\langle\psi_f|\,(T^\dagger - T)\,|\psi_i\rangle\ , \\ \sum_n \langle\psi_f|\, T\,|\psi_n\rangle\,\langle\psi_n|\, T^\dagger\,|\psi_i\rangle &= i(T_{if} - T^*_{if})\,, \\ \sum_n T_{fn}T^*_{in} &= 2\,\text{Im}[T_{if}]\,. \end{aligned} \tag{3.9}$$

The last step is to reduce the identity to the forward scattering amplitude, which means that the initial and the final state have to be the same. Therefore we get

$$\sum_n |T_{in}|^2 = 2\,\text{Im}[T_{ii}]\,. \tag{3.10}$$

Roughly speaking, this implies that the amplitude for an initial state to turn into any state equals two times the imaginary part of a process that has the same initial and final state, but with any intermediate steps in between. For our case of electron-positron annihilation to hadronic matter creation the theorem looks like [7]:

$$\sigma_{e^+/e^-\to\text{hadrons}}(q) = \frac{4\pi\alpha}{q^2}\text{Im}\left[\Pi^{\text{R}}_{\text{had.}}\right]\ . \tag{3.11}$$

3.4 Muon pair production cross section

In an experiment it is rather difficult to measure a total cross section on an absolute scale. Thus it is preferable to use a total cross section in relative units, $R(q^2)$, in this case relative to the total cross section of muon creation:

$$R\left(q^2\right) = \frac{\sigma_{e^+/e^- \to \text{hadrons}}\left(q^2\right)}{\sigma_{e^+/e^- \to \mu^+/\mu^-}\left(q^2\right)}\,. \tag{3.12}$$

The Lorentz-invariant differential cross section for $2 \to 2$ scattering is, according to [8]:

$$d\sigma = \frac{(2\pi)^4}{4E_p E_{p'}|\vec{\nu_p} - \vec{\nu_p'}|}\frac{d^3k}{(2\pi)^3 2E_k}\frac{d^3k'}{(2\pi)^3 2E_{k'}}\delta^{(4)}(p + p' - k - k')|M_{fi}|^2\,, \tag{3.13}$$

with the momenta p, p' and energies E_p, $E_{p'}$ of the incoming particles, the momenta k, k' and energies E_k, $E_{k'}$ of the outgoing particles, and the ratio of the 3-momentum to the energy of a particle $\vec{\nu}_p = \vec{p}/E_p$.The invariant matrix element iM of the $(e^+/e^- \to \mu^+/\mu^-)$-process using Feynman rules reads

$$iM(q^2) = \frac{ie^2}{q^2}\bar{v}_{s'}(p')\gamma^\mu u_s(p)\bar{u}_r(k)\gamma_\mu v_{r'}(k')\,. \tag{3.14}$$

Only the q^2-dependence of the cross section is of interest for us now. Thus, the information on polarization is not needed and the amplitude-square is averaged over incoming and outgoing polarization states. Using the spinor completeness relations, the expression can be written as

$$\begin{aligned}\frac{1}{4}\sum_{s,s',r,r'}|M|^2 = \frac{e^4}{4q^4}\Big[&\mathrm{Tr}\big((\gamma\cdot p - m_e\mathbb{1})\gamma^\mu(\gamma\cdot p + m_e\mathbb{1})\gamma^\nu\big)\\ &\times\mathrm{Tr}\big((\gamma\cdot p + m_\mu\mathbb{1})\gamma_\mu(\gamma\cdot p - m_\mu\mathbb{1})\gamma_\nu\big)\Big]\,.\end{aligned} \tag{3.15}$$

Using trace identities for the γ-matrices, one obtains

$$\frac{1}{4}\sum_{s,s',r,r'}|M|^2 = \frac{8e^4}{q^4}\big[(p\cdot k)(p'\cdot k') + (p\cdot k')(p'\cdot k) \\ +(p\cdot p')m_\mu^2 + (k\cdot k')m_e^2 + 2m_e^2 m_\mu^2\big]\,. \tag{3.16}$$

Now we can switch to the center-of-mass frame to simplify the expression further with the following substitutions:

$$p = \begin{pmatrix} E \\ \vec{p} \end{pmatrix},\ p' = \begin{pmatrix} E \\ -\vec{p} \end{pmatrix},\ k = \begin{pmatrix} E \\ \vec{k} \end{pmatrix},\ \vec{p}\cdot\vec{k} = |\vec{p}||\vec{k}|\cos\theta\,,$$

$$\begin{aligned} q^2 &= (k+k')^2 = (p+p')^2\,, \\ p\cdot k &= p'\cdot k' = E^2 - |\vec{p}||\vec{k}|\cos\theta\,, \\ p\cdot k' &= p'\cdot k = E^2 + |\vec{p}||\vec{k}|\cos\theta\,. \end{aligned} \tag{3.17}$$

The final result for the unpolarized amplitude-square is

$$\frac{1}{4}\sum_{s,s',r,r'}|M|^2 = e^4\left[\left(1+\frac{4m_\mu^2}{q^2}+\frac{4m_e^2}{q^2}\right)+\left(1-\frac{4m_\mu^2}{q^2}-\frac{4m_e^2}{q^2}+\frac{16m_\mu^2 m_e^2}{q^4}\right)\cos^2\theta\right]. \tag{3.18}$$

Further two expressions have to be used:

$$\delta(g(x)) = \sum_{i=1}^{n}\frac{\delta(x-x_i)}{|g'(x_i)|}\,,\ \text{with } x_i \text{ being the zeros of } g(x)\,, \tag{3.19}$$

$$|\nu_p - \nu_{p'}| = \left|\frac{p}{E_p} - \frac{p'}{E_{p'}}\right| = \frac{4|p|}{E_{\text{com}}}\,. \tag{3.20}$$

Plugging Eq. (3.18) into the cross-section formula Eq. (3.13), the total cross section of the $(e^+/e^- \to \mu^+/\mu^-)$-process can be finally written down [9]:

$$\sigma_{e^+/e^-\to\mu^+/\mu^-}(q) = \frac{4\pi\alpha^2}{3q^2}\frac{\sqrt{1-\frac{4m_\mu^2}{q^2}}}{\sqrt{1-\frac{4m_e^2}{q^2}}}\left[\left(1+\frac{2m_\mu^2}{q^2}\right)\left(1+\frac{2m_e^2}{q^2}\right)\right]. \tag{3.21}$$

If m_e is neglected because of $m_\mu \gg m_e$, we can compare the total cross section with the VP function, since both describe only the modification of the photon propagator. Comparing this limit of the total cross section in Eq. (3.21) with the imaginary part of the polarization function from Eq. (3.6), the form of the optical theorem in Eq. (3.11) can be explicitly verified.

In the ultrarelativistic limit with $|\vec{p}| \gg m_\mu$, the cross section is described by a very simple formula:

$$\sigma_{\text{ul.-rel.}} = \frac{4\pi\alpha^2}{3\,q^2}\,. \tag{3.22}$$

Using this limit and the total cross section in relative units, $R(q^2)$, the hadronic polarization function can be written like this [10]:

$$\begin{aligned}
\text{Re}\left[\Pi^{\text{R}}_{had.}\left(q^2\right)\right] &= \frac{q^2}{\pi} P \int_{-\infty}^{+\infty} \frac{\text{Im}\left[\Pi^{\text{R}}\left(q'^2\right)\right]}{q'^2(q'^2 - q^2 - i\epsilon)} dq'^2 \\
&= \frac{q^2}{4\pi^2\alpha} P \int_{4m_\pi^2}^{+\infty} \frac{\sigma_{e^+/e^-\to\text{hadrons}}\left(q'^2\right)}{(q'^2 - q^2 - i\epsilon)} dq'^2 \\
&= \frac{\alpha q^2}{3\pi} P \int_{4m_\pi^2}^{+\infty} \frac{R\left(q'^2\right)}{q'^2(q'^2 - q^2 - i\epsilon)} dq'^2\,,
\end{aligned} \tag{3.23}$$

with m_π being the mass of the lightest hadron, the pion. As a result, to construct the hadronic polarization function, only a total cross section of the hadronic matter created in the pair annihilation process in relative units is needed.

4 Dirac equation in a central potential

In this chapter, a brief introduction to relativistic quantum mechanics is given, focusing on the bound-state solutions of the Dirac equation in a central potential.

4.1 Separation of variables in a central potential

This thesis is about the energy shifts of bound electrons in atoms induced by VP. As an electron is a spin-$\frac{1}{2}$ particle, the correct way to describe it is given by the Dirac equation

$$(i\partial\!\!\!/ - m)\psi(x) = 0\,, \tag{4.1}$$

with the partial derivative ∂ and the wave function $\psi(x)$ of the spin-$\frac{1}{2}$ particle, and the gamma matrices γ^μ that fulfill the Clifford algebra

$$\{\gamma^\mu, \gamma^\nu\} = \gamma^\mu\gamma^\nu + \gamma^\nu\gamma^\mu = 2\eta^{\mu\nu}\,. \tag{4.2}$$

We will look at the Dirac equation in another basis

$$i\frac{d\psi}{dt} = \left(\hat{\beta}m - i\sum_{n=1}^{3}\hat{\alpha}_i\frac{\partial}{\partial x^i}\right)\psi = \left(\hat{\beta}m + \sum_{n=1}^{3}\hat{\alpha}_i\hat{p}_i\right)\psi \equiv \hat{H}_{\mathrm{D}}\psi\,, \tag{4.3}$$

with $\hat{\beta} = \gamma_0$, $\hat{\alpha}_i = \beta\,\gamma_i$, and they fulfill the following identities

$$\begin{aligned}\{\alpha^i, \alpha^k\} = \alpha^i\alpha^k + \alpha^k\alpha^i = 2\delta^{ik}\mathbb{1}\,,\\ \{\alpha^i, \beta\} = \alpha^i\beta + \beta\alpha^i = 0\,,\\ (\alpha^i)^2 = (\beta)^2 = \mathbb{1}\,.\end{aligned} \tag{4.4}$$

The Dirac Hamiltonian of an electron in a central potential $V(r)$ is given by

$$\hat{H}_D = \sum_{n=1}^{3} \hat{\alpha}_i \hat{p}_i + \hat{\beta} m + V(r)\,. \tag{4.5}$$

The approach to rewrite this equation can be seen in length for example in [11]. Here, we outline the most important steps. Due to the spherical symmetry of the potential, the parity and angular momentum operators commute with the Hamilton operator. Therefore, states with defined energy, angular momentum and parity exist. The 4-spinor ψ_{jm} can be written in terms of two 2-spinors, and a separational ansatz can be made because of the spherical symmetry:

$$\psi_{jm}\left(\vec{r}\right) = \begin{pmatrix} \varphi_{jlm}\left(\vec{r}\right) \\ \chi_{jl'm}\left(\vec{r}\right) \end{pmatrix} = \begin{pmatrix} ig(r)\Omega_{jlm}\left(\vec{r}/r\right) \\ -f(r)\Omega_{jl'm}\left(\vec{r}/r\right) \end{pmatrix}, \tag{4.6}$$

with the spherical spinor Ω_{jlm}, and $l' = 2j - l$ to ensure different parity for the small and large components. The Ω_{jlm} is an eigenfunction of the angular momentum and parity operators, and fulfills the following identity:

$$\left(\sum_{n=1}^{3} \hat{\sigma}_i r_i\right) \frac{\Omega_{jlm}}{r} = -\Omega_{jl'm}\,. \tag{4.7}$$

The following representation of $\hat{\alpha}_i$ and $\hat{\beta}$ are used:

$$\begin{aligned} \hat{\alpha}_i &= \begin{pmatrix} 0 & \hat{\sigma}_i \\ \hat{\sigma}_i & 0 \end{pmatrix}, \\ \hat{\beta} &= \begin{pmatrix} \mathbb{1}_{2x2} & 0 \\ 0 & -\mathbb{1}_{2x2} \end{pmatrix}, \end{aligned} \tag{4.8}$$

with the Pauli matrices $\hat{\sigma}_i$. Thereby, our stationary Dirac equation $\hat{H}_{\mathrm{D}}\psi = E\psi$ can be written as

$$
\begin{aligned}
(E - m - V(r))\,\varphi_{jlm} &= \left(\sum_{n=1}^{3} \hat{\sigma}_i \hat{p}_i\right) \chi_{jl'm}\,, \\
(E + m - V(r))\,\chi_{jl'm} &= \left(\sum_{n=1}^{3} \hat{\sigma}_i \hat{p}_i\right) \varphi_{jlm}\,.
\end{aligned} \tag{4.9}
$$

We can rewrite the right side by inserting the ansatz from Eq. (4.6) and using the identity from Eq. (4.7):

$$
\begin{aligned}
\left(\sum_{n=1}^{3} \hat{\sigma}_i \hat{p}_i\right) \varphi_{jlm} &= \frac{dg(r)}{dr} \left(\sum_{n=1}^{3} \hat{\sigma}_i r_i\right) \frac{\Omega_{jlm}}{r} + ig(r) \left(\sum_{n=1}^{3} \hat{\sigma}_i \hat{p}_i\right) \Omega_{jlm} \\
&= -\frac{dg(r)}{dr} \Omega_{jl'm} - g(r) \left(\frac{2}{r} + \frac{1}{r} \left(\sum_{n=1}^{3} \hat{L}_i \hat{\sigma}_i\right)\right) \Omega_{jl'm}\,.
\end{aligned} \tag{4.10}
$$

This can be simplified by introducing a new operator for which the spherical spinors are eigenfunctions as well:

$$
\begin{aligned}
&\hat{\kappa} = 1 + \left(\sum_{n=1}^{3} \hat{L}_i \hat{\sigma}_i\right)\,, \\
&\hat{\kappa} \chi_{\kappa m} = -\kappa \chi_{\kappa m}\,,
\end{aligned}
$$

$$
\text{with } \kappa = \begin{cases} -(j + \frac{1}{2}) = -(l+1), & \text{for } j = l + \frac{1}{2}\,, \\ +(j + \frac{1}{2}) = l, & \text{for } j = l - \frac{1}{2}\,. \end{cases} \tag{4.11}
$$

Hence, we get for Eq. (4.10) and in an analogous calculation for the other spinor component

$$
\begin{aligned}
\left(\sum_{n=1}^{3} \hat{\sigma}_i \hat{p}_i\right) \varphi_{jlm} &= -\Omega_{jl'm} \left(\frac{dg(r)}{dr} + \frac{(\kappa+1)}{r} g(r)\right)\,, \\
\left(\sum_{n=1}^{3} \hat{\sigma}_i \hat{p}_i\right) \chi_{jl'm} &= -i\Omega_{jlm} \left(\frac{df(r)}{dr} - \frac{(\kappa-1)}{r} f(r)\right)\,.
\end{aligned} \tag{4.12}
$$

By inserting these relations into Eq. (4.9), the spinors cancel each other. Now the differential equations for the radial functions can be written as

$$\begin{aligned} \frac{dg(r)}{dr} + (1+\kappa)\frac{g(r)}{r} - \big(E + m - V(r)\big)f(r) = 0\,, \\ \frac{df(r)}{dr} + (1-\kappa)\frac{f(r)}{r} - \big(E - m - V(r)\big)g(r) = 0\,. \end{aligned} \tag{4.13}$$

The usual representation of the differential equations is achieved by applying the following substitutions:

$$G(r) \equiv r g(r)\,, \qquad\qquad F(r) \equiv r f(r)\,. \tag{4.14}$$

Now the coupled radial differential equations read

$$\begin{aligned} \frac{dG(r)}{dr} + G(r)\frac{\kappa}{r} - \big(E + m - V(r)\big)F(r) = 0\,, \\ \frac{dF(r)}{dr} - F(r)\frac{\kappa}{r} - \big(E - m - V(r)\big)G(r) = 0\,. \end{aligned} \tag{4.15}$$

4.2 Radial solutions in a Coulomb potential

The Dirac equation in a Coulomb potential can be solved analytically for a point-like nucleus. The potential is given by

$$V(r) = -\frac{Z\alpha}{r}\,. \tag{4.16}$$

The approach to solve these equations is given at length in [11] and [12]. We are interested in the solutions to calculate and compare energy shifts. The solutions are given by

$$\left.\begin{matrix} g_{n\kappa}(r) \\ f_{n\kappa}(r) \end{matrix}\right\} = N\sqrt{m \pm E}\, e^{-\lambda r}(2\lambda r)^{\gamma-1}(2\lambda) \tag{4.17}$$
$$\times\left[{}_1F_1(1-n+|\kappa|, 2\gamma+1; 2\lambda r) \pm \frac{1}{n-|\kappa|}\left(\kappa - \frac{Z\alpha m}{\lambda}\right){}_1F_1(-n+|\kappa|, 2\gamma+1; 2\lambda r)\right],$$

with n, λ, γ and the confluent hypergeometric function ${}_1F_1(a, c; x)$ given by

$$\begin{aligned} n &= 1, 2, 3, \dots, \\ \lambda &\equiv \sqrt{m^2 - E^2}\,, \\ \gamma &\equiv \sqrt{\kappa^2 - (Z\alpha)^2}\,, \\ {}_1F_1(a, b; x) = \sum_{n=0}^{\infty} \frac{a_n\, x^n}{c_n\, n!} &= 1 + \sum_{n=1}^{\infty} \frac{a(a+1)\dots(a+n-1)x^n}{c(c+1)\dots(c+n-1)n!}\,. \end{aligned} \tag{4.18}$$

For the energy eigenvalue $E_{n\kappa}$ we get

$$E_{n\kappa} = m\left[1 + \frac{(Z\alpha)^2}{\left(n - |\kappa| + \gamma\right)^2}\right]^{-1/2}. \tag{4.19}$$

The wave function can be normalized by the condition

$$\int_0^\infty \left(G^2_{n\kappa}(r) + F^2_{n\kappa}(r)\right) dr = \int_0^\infty \left(g^2_{n\kappa}(r) + f^2_{n\kappa}(r)\right) r^2 dr = 1\,. \tag{4.20}$$

For this condition, we get the normalization constant

$$N = -\frac{\lambda^{3/2}(n-|\kappa|)}{\Gamma(2\gamma+1)}\left(\frac{\Gamma(2\gamma+n-|\kappa|+1)}{2Z\alpha m^2(-\lambda\kappa + Z\alpha m)(n-|\kappa|)!}\right)^{1/2}. \tag{4.21}$$

Thus, the complete solutions for $g(r)$ and $f(r)$ in a Coulomb field are

$$\left.\begin{matrix} g_{n\kappa}(r) \\ f_{n\kappa}(r) \end{matrix}\right\} = \frac{\sqrt{2}\,\lambda^{5/2}}{\Gamma(2\gamma+1)}\left(\frac{\Gamma(2\gamma+n-|\kappa|+1)(m \pm E)}{(n-|\kappa|)!\, Z\alpha m^2(Z\alpha m - \lambda\kappa)}\right)^{1/2} e^{-\lambda r}(2\lambda r)^{\gamma-1} \tag{4.22}$$
$$\times\left[-(n-|\kappa|){}_1F_1(1-n+|\kappa|, 2\gamma+1; 2\lambda r) \mp \left(\kappa - \frac{Z\alpha}{\lambda}\right){}_1F_1(-n+|\kappa|, 2\gamma+1; 2\lambda r)\right].$$

Since the Uehling potential is only important for small radii away from the origin, our evaluation will focus on the $1S_{1/2}$ wave function which has the largest contribution near the origin. This state is given by

$$\begin{aligned} n &= 1\,, \\ \kappa &= -1\,, \\ {}_1F_1(-n+|\kappa|, 2\gamma+1; 2\lambda r) &= {}_1F_1(0, 2\gamma+1; 2\lambda r) = 1\,. \end{aligned} \tag{4.23}$$

For this state the wave functions simplify to

$$\left.\begin{matrix} g(r) \\ f(r) \end{matrix}\right\} = \pm\sqrt{2}\,\lambda^{3/2}\left(\frac{(m\pm E)(Z\alpha m+\lambda)}{\Gamma(2\gamma+1)Z\alpha m^2}\right)^{1/2} e^{-\lambda r}(2\lambda r)^{\gamma-1}\,. \tag{4.24}$$

The $1S_{1/2}$-wave functions $G(r)$ and $F(r)$ are plotted in the figure below.

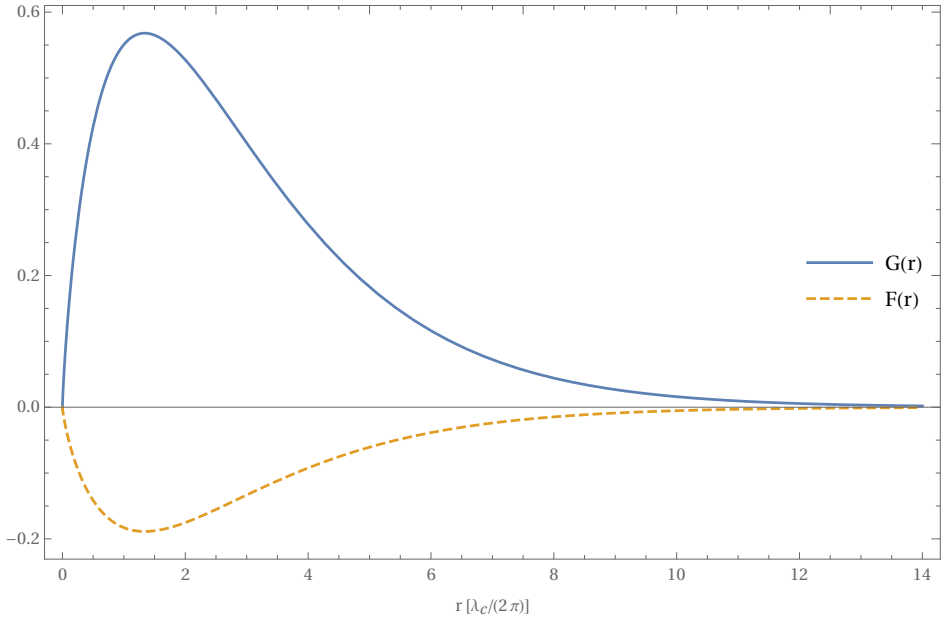

Figure 4.1: Radial wave functions $G(r)$ and $F(r)$ plotted against the radius r in units of the reduced Compton wavelength of the electron.

5 Hadronic vacuum polarization

5.1 Parameterized hadronic polarization function

As discussed in chapter 3, the hadronic polarization function can be constructed with experimental collision data. This was done for example by Burkhardt and collaborators [7], who used data from different experiments and energy regions, and also gave an approximate parametrization for the polarization function

$$\mathrm{Re}\left[\Pi_{\mathrm{had.}}\left(q^2\right)\right] = A_i + B_i \ln\left(1 + C_i \left|q^2\right|\right) , \tag{5.1}$$

with three constants A_i, B_i, C_i, that are given for different q^2-regions. For our evaluation, an updated version of this parametrization with more energy regions will be used, as given in [13].

Region	Range [GeV]	A_i	B_i	C_i
$0 - k_1$	$0.0 - 0.7$	0.0	0.0023092	3.9925370
$k_1 - k_2$	$0.7 - 2.0$	0.0	0.0022333	4.2191779
$k_2 - k_3$	$2.0 - 4.0$	0.0	0.0024402	3.2496684
$k_3 - k_4$	$4.0 - 10.0$	0.0	0.0027340	2.0995092
$k_4 - k_5$	$10.0 - m_Z$	0.0010485	0.0029431	1.0
$k_5 - k_6$	$m_Z - 10^4$	0.0012234	0.0029237	1.0
$k_6 - k_7$	$10^4 - 10^5$	0.0016894	0.0028984	1.0

Table 5.1: Parameters for the parameterization from Eq. (5.1) of the hadronic polarization function given in [13], with the mass of the Z boson m_Z

The first four energy regions ($k_0 - k_4$) of the in total seven are plotted in the following figure.

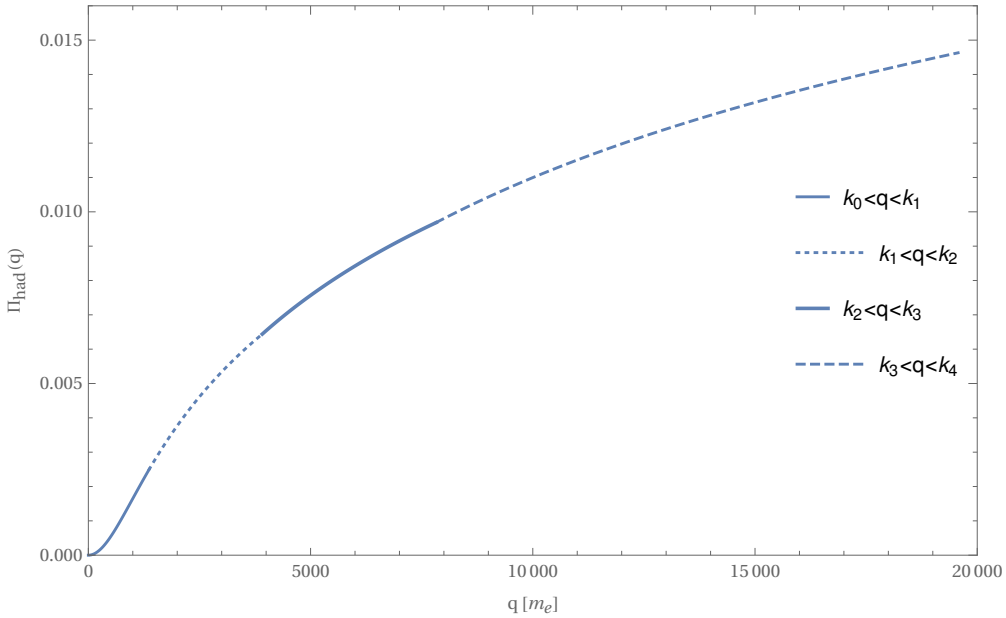

Figure 5.1: Parameterized hadronic VP function plotted against the impulse q in units of the electron mass m_e, with parameters taken from [13].

5.2 Hadronic Uehling potential

The Uehling potential for this parameterization is therefore given by

$$A_0^{\text{mod}}(\vec{x}) = \sum_{i=1}^{7} \left[-Ze \int_{k_{i-1}}^{k_i} \frac{d^3q}{(2\pi)^3} e^{i\vec{q}\cdot\vec{x}} \frac{4\pi}{\vec{q}^2} \tilde{\rho}(\vec{q}) \left[1 + A_i + B_i \ln(1 + C_i|q^2|)\right] \right]. \tag{5.2}$$

For a spherical $\tilde{\rho}(\vec{q})$, the angular integrations can be performed easily in spherical coordinates:

$$A_0^{\text{mod}}(r) = -Ze\frac{2}{\pi} \sum_{i=1}^{7} \left[\int_{k_{i-1}}^{k_i} d|q|\, j_0(|q|r) \left[1 + \mathrm{A}_i + \mathrm{B}_i \ln(1 + \mathrm{C}_i|q|^2)\right] \tilde{\rho}(|q|) \right], \tag{5.3}$$

with $r \equiv |\vec{x}|$, $|q| \equiv |\vec{q}|$ and the spherical Bessel function of first kind $j_0(x) = \text{sinc}(x) = \frac{\sin(x)}{x}$. For a point-like nucleus ($\tilde{\rho}(\vec{q}) = 1$) we can solve the integral in the boundaries from zero to infinity to get a intuition for the integral using the dummy constants A, B and C that are supposed to apply for the whole integration region:

$$
\begin{aligned}
&- Ze\frac{2}{\pi}\int_0^\infty d|q|\,\frac{\sin(|q|r)}{|q|r}\left[1+A+B\ln(1+C|q|^2)\right] \\
=&-\frac{Ze}{r}\left[1+A+2BE_1\left(\frac{r}{\sqrt{C}}\right)\right], \\
&\text{with } E_1(x)=-\int_{|x|}^\infty dt\frac{e^{-t}}{t}\,.
\end{aligned}
\tag{5.4}
$$

This shows the Coulomb potential is corrected by the constant A and the expression with the exponential integral E_1 shows a similar asymptotic behavior to the potential induced purely by VP. For our given boundaries k_i, the Coulomb-like part of the integral can be evaluated, but no direct analytical solution for the integral of the logarithm was found. However, the sinc-function can be expanded as a Taylor series, making also the logarithm part integrable, assuming that summation and integration can be exchanged:

$$
\begin{aligned}
A_0^{\text{mod}}(r) =& - Ze\frac{2}{\pi}\sum_{i=1}^{7}\left(\left[(1+A_i)\frac{\text{Si}(|q|r)}{r}\right]_{k_{i-1}}^{k_i}\right. \\
&\left.+\int_{k_{i-1}}^{k_i} d|q|\sum_{n=0}^{\infty}\frac{(-(|q|r)^2)^n}{(2n+1)!}\left[B_i\ln(1+C_i|q|^2)\right]\right) \\
\\
=& - Ze\frac{2}{\pi}\sum_{i=1}^{7}\left(\left[(1+A_i)\frac{\text{Si}(k_ir)-\text{Si}(k_{i-1}r)}{r}\right]\right. \\
&+\left[\sum_{n=0}^{\infty}\frac{B_i\,|q|\,(-(|q|r)^2)^n}{(2n+1)!(2n+1)^2}\right. \\
&\left.\left.\times\left[-2+2{}_2F_1(1,\frac{1}{2}+n;\frac{3}{2}+n;-C_i|q|^2)+(1+2n)\ln(1+C_i|q|^2)\right]\right]_{k_{i-1}}^{k_i}\right),
\end{aligned}
\tag{5.5}
$$

with the sine integral $\text{Si}(x)$ and the ordinary hypergeometric function ${}_2F_1(a,b;c;x)$ given by

$$\mathrm{Si}(x) = \int_0^z dt \frac{\sin t}{t}\,,$$
$$ {}_2F_1(a,b;c;x) = \sum_{n=0}^{\infty} \frac{a_n b_n\, x^n}{c_n\, n!} = 1 + \sum_{n=1}^{\infty} \frac{a...(a+n-1)b...(b+n-1)x^n}{c(c+1)...(c+n-1)n!}\,. \tag{5.6}$$

This expression converges very slowly for large values of $|q|r$. Therefore, this method is neglected and the numerical integration routine from Mathematica is used instead which produces good results.

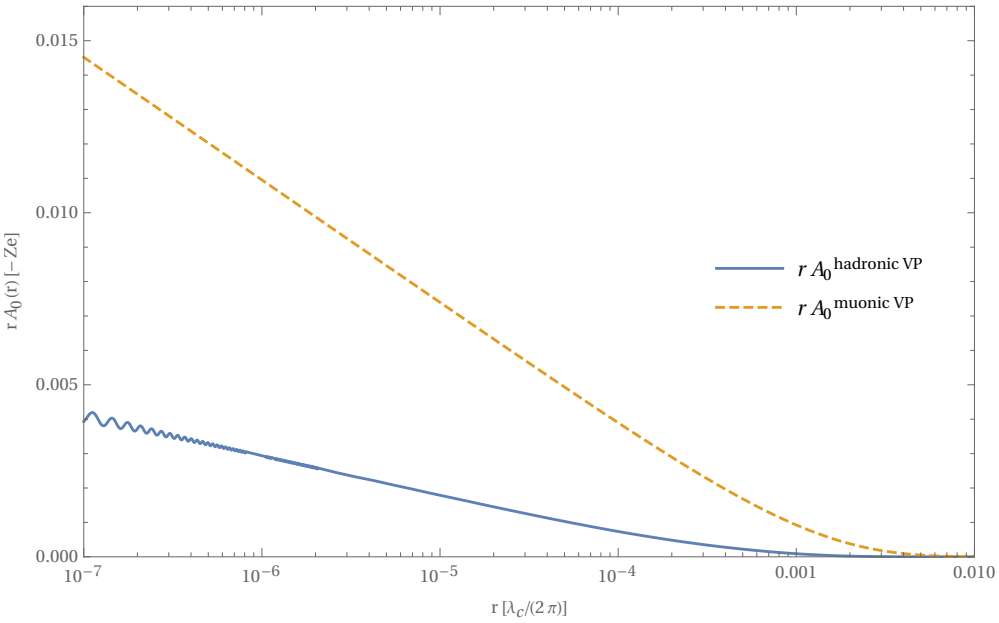

Figure 5.2: Muonic and hadronic Uehling potential divided by the Coulomb potential plotted against the radius r in units of the reduced Compton wavelength of the electron.

In figure (5.2) the muonic Uehling potential is compared to the hadronic Uehling potential. It also possesses a logarithmic divergence for small radii, but the gradient is not as steep as for the muonic Uehling potential. At about $10^{-6}\,\lambda_C/(2\pi)$ and below, an oscillation of the potential becomes visible. This effect is caused by the finite integration limit that was given in the parameterization, respectively the finite number of modes used to describe the function. The effect is only visible for very small radii but poses problems with the numerical integration. One possibility to deal with this effect is to raise the

highest integration limit, thereby shifting it to even smaller radii. Another possibility turns up naturally in the next section, when a finite nuclear radius is considered.

5.3 Hadronic Uehling potential for finite nuclear sizes

The muonic VP is already very sensitive to finite nuclear size effects, and this applies even more to the hadronic effect. Since the numerical integration for the hadronic Uehling potential already demands more computing time than the leptonic Uehling potential, a very simple model of a homogeneously charged nucleus is chosen. This is given by the charge density

$$\rho(x) = \begin{cases} \frac{3}{4\pi R^3}, & \text{for } x \leq R\,, \\ 0, & \text{for } x > R\,, \end{cases} \tag{5.7}$$

with R being the radius of the nucleus. The Fourier transform of the charge density is

$$\tilde{\rho}\,(|q|) = 3\left(\frac{\sin(|q|R) - |q|R\cos(|q|R)}{|q|^3 R^3}\right) = \frac{3j_1(|q|R)}{|q|R}\,, \tag{5.8}$$

with the spherical Bessel function $j_1(x)$.

In figure 5.3 the effect of the finite nuclear size on the Uehling potential can be seen. The divergence at the origin vanishes and additionally the oscillations induced by the finite integration limit are largely suppressed.

5.4 Energy level shifts for the hadronic Uehling potential

The energy correction in an atom due to hadronic VP can be approximated by treating it as a small perturbation to the Dirac-Coulomb wave function of a finite nucleus. The first perturbative order is given by

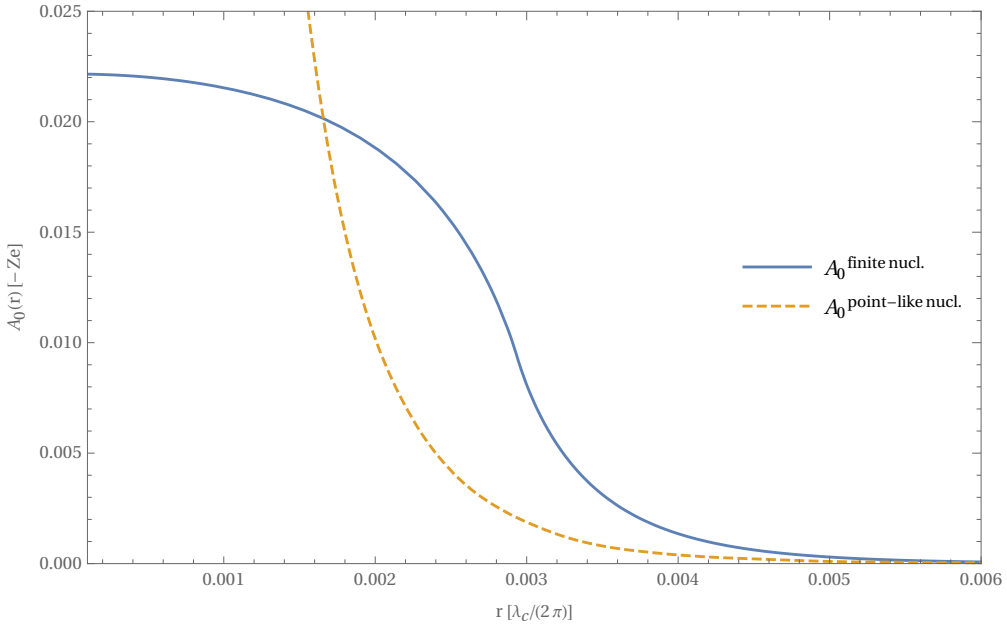

Figure 5.3: Hadronic Uehling potential with point-like and finite nucleus divided by the Coulomb potential plotted against the distance r in units of the reduced Compton wavelength of the electron.

$$
\begin{aligned}
\Delta E^{\text{had. VP, CD}}_{\text{rel., }1^{\text{st}}\text{-order}} &= \langle \psi_{n\kappa' m'} |\, V(\vec{x}) \,| \psi_{n\kappa m} \rangle \\
&= \int_0^\infty dr\, V(r) \big(G^2_{n\kappa}(r) + F^2_{n\kappa}(r) \big) \delta_{\kappa\kappa'} \delta_{mm'} \\
&= \int_0^\infty dr\, V(r) \big(g^2_{n\kappa}(r) + f^2_{n\kappa}(r) \big) r^2 \,, \\
\text{with} \quad \int_0^\pi d\vartheta \int_0^{2\pi} d\varphi\, \Omega^\dagger_{\kappa' m'}(\vartheta, \varphi) \Omega_{\kappa m}(\vartheta, \varphi) &= \delta_{\kappa\kappa'} \delta_{mm'}
\end{aligned}
\tag{5.9}
$$

using the Dirac-Coulomb wave functions.
To test the energy values for low values of Z and thereby at low energies, the logarithm in the polarization function can be approximated with the first non-constant element of its Taylor series. For this approximation only the first energy region of parameterization has to be used, therefore only the parameters A_1, B_1 and C_1 are needed and we obtain for our Uehling potential with a point-like nucleus:

$$A_0^{\text{VP had.}}(\vec{x}) = -Ze\left(\frac{1}{|\vec{x}|} + 4\delta^{(3)}(\vec{x})B_1C_1\right)$$
$$= A_0^{\text{Coulomb}}(\vec{x}) + A_0^{\text{VP had.}}(\vec{x})\,. \tag{5.10}$$

The energy shift induced by the hadronic VP can be calculated using the analytical non-relativistic Coulomb-wave functions to yield

$$\Delta E^{\text{had. VP}}_{\text{non-rel.}} = \langle\Psi_{nl}|\, A_0^{\text{VP had.}}(\vec{x})\,|\Psi_{nl}\rangle = \frac{-4(Z\alpha)^4 m^3}{n^3} B_1C_1\,,$$
$$\text{with } |\Psi_{nl}(\vec{x}=0)|^2 = \frac{m^3(Z\alpha)^3}{\pi n^3}\delta_{l0}\,. \tag{5.11}$$

This formula agrees with that of Friar et al. [14]. Numerical results are presented in the next chapter.

6 Results

At first we calculate the hadronic energy shift $\Delta E^{\text{had. VP}}_{\text{non-rel.}}$ for hydrogen with the non-relativistic approximation from Eq. (5.11). This is performed to have a reference for the later more complicated approaches, and because this approximation is expected to be a good estimation for hydrogen. The result is

$$\begin{aligned} \Delta E^{\text{had. VP}}_{\text{non-rel.}} &= -1.39538 \times 10^{-11}\ \text{eV} \\ &= 0.66465\, \Delta E^{\text{muonic VP}}_{\text{non-rel.}}\,, \end{aligned} \tag{6.1}$$

with the energy shift due to muonic VP $\Delta E^{\text{muonic VP}}_{\text{non-rel.}}$. This is in good agreement with $\Delta E^{\text{had. VP}}_{\text{non-rel.}} = 0.671(15)\Delta E^{\text{muonic VP}}_{\text{non-rel.}}$ from [14], with the difference stemming from using newer experimental constants B_1 and C_1 in Eq. (5.11) as compared to [14]. The hydrogenic systems for which we will show the computed energy shifts induced by hadronic VP are:

Element	Z	R_{rms} [fm]
^{1}H	1	0.8783(86)
^{28}Si	14	3.1224(24)
^{40}Ca	20	3.4776(19)
^{208}Pb	82	5.5012(13)

Table 6.1: Hydrogenic ions used in this thesis with the mass number and element acronym ^{A}X, the charge number Z and the root-mean-square radius of the nucleus, R_{rms}. The latter are taken from [15].

The computation of the hadronic VP energy shift for point-like nuclei demonstrates a problem of the finite definition of the polarization function parameterization. The oscillation of the hadronic Uehling potential, visible in figure (5.2), began only at very small radii (10^{-3} fm). However, our numerical routine does not converge for the given integration limit of 10^5 GeV, and even for artificial higher integration limits, the additional contributions are not negligible. When the effect of a finite nucleus is included

these problems do not appear and the integration routine converges. Depending on the charge number, five to six of the seven parametrized energy sections are necessary for the integral to converge for our desired level of accuracy. Additionally, for lead ($Z = 82$) the energy shift was computed numerically with bound Dirac-Coulomb wave functions corresponding to a finite nucleus. This was necessary since there are no analytical solutions for a spherical homogeneous charged nucleus, but the effect of the finite nucleus for lead and other heavy elements is non-negligible at our accuracy. The numerical wave functions were computed using a computer code developed by Robin Weis for his Bachelor thesis [16]. The numerical method is described in detail in [17]. The approach of this method is to find solutions for very small and for very large radii where the coupled radial differential equations simplify. The two solutions are then evaluated at a matching point and their differences are minimized iteratively.

Non-perturbative, i.e. all-order numerical results for the exact wave functions induced by the hadronic Uehling potential were provided by Halil Cakir [18]. He wrote a computer code that approximates the real wave function using a spline representation. To this end, the values of the Uehling potential at 1980 respectively 3960 specified points were used to compute the energy shift by adding the Uehling potential to the nuclear Coulomb potential in the radial Dirac equation. The results are shown in table (6.2).

Z	$\Delta E^{\text{had. VP}}_{\text{non-rel.}}$ [eV]	$\Delta E^{\text{had. VP, CD}}_{\text{rel., 1}^{\text{st}}\text{-order}}$ [eV]	$\Delta E^{\text{had. VP, NS}}_{\text{rel., exact}}$ [eV]
1	-1.39538×10^{-11}	$-1.4055(18) \times 10^{-11}$	$-1.3909(39) \times 10^{-11}$
14	-5.36048×10^{-7}	$-5.78119(1) \times 10^{-7}$	$-5.75605(72) \times 10^{-7}$
20	-2.23260×10^{-6}	$-2.582522(2) \times 10^{-6}$	$-2.55961(31) \times 10^{-6}$
82	-6.30881×10^{-4}	$-4.55029(47) \times 10^{-3}$	$-3.6929(37) \times 10^{-3}$

Table 6.2: Energy shift results in the non-relativistic approach $\Delta E^{\text{had. VP}}_{\text{non-rel.}}$, 1^{st}-order perturbation theory with Dirac-Coulomb wave functions $\Delta E^{\text{had. VP, CD}}_{\text{rel., 1}^{\text{st}}\text{-order}}$ and exact wave function of the hadronic Uehling potential for a finite-size nucleus $\Delta E^{\text{had. VP, NS}}_{\text{rel., exact}}$, respectively, for the considered hydrogenic systems.

Additionally, the result for lead computed as a 1^{st}-order perturbation with Dirac-Coulomb wave functions of a finite-size nucleus is

$$\Delta E^{\text{had. VP, FN}}_{\text{rel., } 1^{\text{st}}\text{-order}} = -3.69799(41) \times 10^{-3} \text{ eV} \,. \tag{6.2}$$

The errors given in table (6.2) and Eq. (6.2) are only based on the convergence of the results and the uncertainty of the nuclear root-mean-square radii. The uncertainty coming from the parametrization of the polarization function is difficult to estimate but it probably dominates over the other errors for all elements. Checking the consistency of the different approaches, it is estimated that the first two digits are stable and the second decimal place is fluctuating, i.e. the relative numerical accuracy is expected to be on the level of 1%.
Comparing the non-relativistic results with the other results, one finds that the results for $Z = 1$ agree with each other within our estimated error. For increasing values of Z, the difference increases up to an order of magnitude for $Z = 82$, implying that all considered ions except hydrogen demand a relativistic description. The differences between the results for the 1^{st}-order perturbation of Dirac-Coulomb wave functions and the results for the exact wave function of the hadronic Uehling potential for a finite nucleus coincide within the estimated uncertainty. The exact result for lead however deviates strongly from the 1^{st}-order pertubation of Dirac-Coulomb wave functions. The energy shift for lead can only be described satisfyingly with a wave function of an extended nucleus. Our perturbative result of 1^{st}-order from Eq. (6.2) matches the exact result within the expected uncertainty. Such a good applicability of perturbation theory is not surprising, given the smallness of the perturbation (≈ 4 meV) compared to the binding energy of the electron (≈ 90 keV).
Although the hadronic VP in lead leads to the highest energy shift for the considered ions, even the two-loop QED corrections computed to be around -0.7 eV [19], can not be resolved experimentally yet in the corresponding $2p \to 1s$ x-ray transition [20]. Therefore, we consider another system that could feature measurable shifts, namely, muonic hydrogen.

The results for muonic hydrogen, that are listed in table (6.3), show only a small deviation for the non-relativistic approach for a point-like nucleus compared to the relativistic approaches. The relativistic effects are small due to $Z\alpha \ll 1$.

Z	$\Delta E_{\text{non-rel.}}$ [eV]	$\Delta E^{\text{Cou.-Dirac}}_{\text{rel., 1-order}}$ [eV]	$\Delta E^{\text{finite nucl.}}_{\text{rel., exact}}$ [eV]
1	-1.23351×10^{-4}	$-1.224159(93) \times 10^{-4}$	$-1.2212(10) \times 10^{-4}$

Table 6.3: Results for non-relativistic approach, 1^{st}-order perturbation theory with Dirac-Coulomb wavefunctions and exact wavefunction of the hadronic Uehling potential for a finite nucleus for muonic hydrogen.

7 Summary and outlook

The rising precision of both experimental spectroscopic measurements and theoretical predictions calls for more detailed description of known effects. The muonic VP is already an established part of theory [21]. The hadronic VP has already been considered in precision calculations, i.e. [21], but these evaluations use the non-relativistic approximation from Friar et al. [14]. In order to assure that the hadronic VP does not limit the precision of theory, a generalized approach is desirable. In this approach we take into account relativistic effects, which are relevant in highly charged ions like in [1], and the finite nuclear size effects, which are important in heavy ions such as lead. Therefore this thesis is a contribution to understand and diminish the uncertainty induced by hadronic vacuum polarization in atomic precision measurements.

In this thesis we examined the properties of the hadronic VP function, and described a different approach on how to obtain a VP function from experimental cross section data, in contrast to the leptonic VP being completely described by the lepton mass and the fine-structure constant. An effective potential was determined by using a parameterized hadronic VP function. Finally, energy shifts induced by the hadronic Uehling potential were computed by using different methods, including a non-relativistic approach, 1^{st}-order perturbation theory with Dirac-Coulomb wave functions, and 1^{st}-order perturbation theory with wave functions for finite nucleus sizes and compared these with the energy shifts computed with exact wave functions of the hadronic Uehling potential for a finite nucleus. The energy shifts were determined for four different H-like systems: H, Si, Ca, and Pb. The results for the energy shift induced by hadronic VP exhibit that for our desired level of accuracy, it is sufficient to describe H non-relativistically, Si and Ca with analytical Dirac-Coulomb wave functions and Pb with relativistic wave functions for finite nuclear sizes. The results calculated with different methods coincided within their estimated area of applicability, the main uncertainty being due to uncertainties in the parameterization of the empirical hadronic VP function. This could be improved in future by using perturbative QCD (pQCD) in the high-energy regime, reducing the problems

discussed due to this parameterization. In [10], the pQCD approach was applied and the scope of application for pQCD in this paper was denoted with > 2.5 GeV. However, the low-energy regime provides the main contribution and can not be dealt with pQCD. An advanced parameterization of the polarization function and more accurate hadronic cross section measurements can improve this area. Not only the description of atomic systems benefits from a better hadronic polarization function, but also the description of scattering processes and free-particle properties such as the free-muon and free-electron g-factor. Another possible enhancement for the approach in this thesis is a more realistic nuclear model than the homogeneously charged sphere, e.g. applying a Fermi-Dirac-distribution for the nuclear charge. This is especially important for muonic atoms, because a large fraction of the wave functions is located inside the nucleus. Fast converging numerical methods for effective potentials that consider the Fermi-Dirac-distribution already exist for leptonic VP [22] and could be adjusted for hadronic VP.

In this thesis we evaluated the impact of hadronic VP effects on the energy levels of an atom. Another possible application is the effect on the bound lepton g-factor induced by hadronic VP. This can be evaluated by taking into account the change of the large and small components of the wave function due to an external magnetic field, and considering the hadronic VP correction of the photon propagator. Nowadays, the g-factor of highly charged ions can be measured to high precision, on the 10^{-11} level [1]. Closely related is the hyperfine splitting of energy levels that is caused by the nuclear magnetic moment. Measurements on the hyperfine splitting probe the atomic wave function on the distance scale of the nucleus, therefore, VP effects are much more pronounced than in case of fine-structure transitions or the level energies considered in the current thesis. These effects could be evaluated in a similar way. A recent laser spectroscopic measurement of the hyperfine splitting in H- and Li-like Bi ions at the GSI revealed discrepancy of theory and experiment [23], indicating that either a thorough re-evaluation or extension of QED calculations are needed, or the nuclear parameters entering the theoretical model need to be re-examined.

Bibliography

[1] S. Sturm, A. Wagner, B. Schabinger, J. Zatorski, Z. Harman, W. Quint, G. Werth, C. H. Keitel, and K. Blaum. g Factor of Hydrogenlike $^{28}Si^{13+}$. *Phys. Rev. Lett.*, 107:023002, 2011.

[2] S. Sturm, F. Köhler, J. Zatorski, A. Wagner, Z. Harman, G. Werth, W. Quint, C. H. Keitel, and K. Blaum. High-precision measurement of the atomic mass of the electron. *Nature*, 506(7489):467–470, 2014.

[3] V. A. Yerokhin, E. Berseneva, Z. Harman, I. I. Tupitsyn, and C. H. Keitel. g Factor of Light Ions for an Improved Determination of the Fine-Structure Constant. *Phys. Rev. Lett.*, 116:100801, 2016.

[4] S. G. Karshenboim. Muonic vacuum polarization contribution to the energy levels of atomic hydrogen. *J. Phys. B*, 28(4):L77, 1995.

[5] W. Greiner and J. Reinhardt. *Theoretische Physik Band 7: Quantenelektrodynamik.* Verlag Harri Deutsch, Thun und Frankfurt am Main, 1984.

[6] Z. Harman. Lecture material for Advanced Quantum Theory, 2017.

[7] H. Burkhardt, F. Jegerlehner, G. Penso, and C. Verzegnassi. Uncertainties in the hadronic contribution to the qed vacuum polarization. *Phys. C*, 43(3):497–501, 1989.

[8] T. Weigand. Lecture notes for Quantum Field Theory I + II, 2014.

[9] N. Borghini. Lecture materials for Grundlagen der Elementarteilchenphysik, 2014.

[10] F. Jegerlehner. Hadronic contributions to the photon vacuum polarization and their role in precision physics. *J. Phys. G*, 29(1):101, 2003.

[11] W. Greiner. *Theoretische Physik Band 6: Relativistische Quantenmechanik – Wellengleichungen.* Verlag Harri Deutsch, Thun und Frankfurt am Main, 1987.

[12] E. M. Rose. *Relativistische Elektronen-Theorie*, volume I. Hochschultaschebücher-Verlag, Mannheim Wien Zürich, 1971.

[13] H. Burkhardt and B. Pietrzyk. Update of the hadronic contribution to the QED vacuum polarization. *Physics Letters B*, 513(1):46 – 52, 2001.

[14] J. L. Friar, J. Martorell, and D. W. L. Sprung. Hadronic vacuum polarization and the Lamb shift. *Phys. Rev. A*, 59:4061–4063, 1999.

[15] I. Angeli and K.P. Marinova. Table of experimental nuclear ground state charge radii: An update. *Atomic Data and Nuclear Data Tables*, 99(1):69 – 95, 2013.

[16] R. Weis. Myonische Vakuumpolarisationskorrekturen zum g-Faktor eines gebundenen Elektrons. Bachelor's thesis, University of Heidelberg, 2014.

[17] R. R. Silbar and T. Goldman. Solving the radial Dirac equations: A Numerical odyssey. *Eur. J. Phys.*, 32:217–233, 2011.

[18] H. Cakir, private communication (2018).

[19] V. A. Yerokhin, P. Indelicato, and V. M. Shabaev. Evaluation of the two-loop self-energy correction to the ground state energy of H-like ions to all orders in $Z\alpha$. *Eur. Phys. J. D*, 25(3):203–238, 2003.

[20] A. Gumberidze, Th. Stöhlker, D. Banaś, K. Beckert, P. Beller, H. F. Beyer, F. Bosch, S. Hagmann, C. Kozhuharov, D. Liesen, F. Nolden, X. Ma, P. H. Mokler, M. Steck, D. Sierpowski, and S. Tashenov. Quantum Electrodynamics in Strong Electric Fields: The Ground-State Lamb Shift in Hydrogenlike Uranium. *Phys. Rev. Lett.*, 94:223001, Jun 2005.

[21] N. A. Belov, B. Sikora, R. Weis, V. A. Yerokhin, S. Sturm, K. Blaum, C. H. Keitel, and Z. Harman. Muonic vacuum polarization correction to the bound-electron g-factor. *ArXiv Atomic Physics*, 2016. arXiv:1610.01340v1 [physics.atom-ph].

[22] L. W. Fullerton and G. A. Rinker. Accurate and efficient methods for the evaluation of vacuum-polarization potentials of order $Z\alpha$ and $Z\alpha^2$. *Phys. Rev. A*, 13:1283–1287, 1976.

[23] J. Ullmann, Z. Andelkovic, C. Brandau, A. Dax, W. Geithner, C. Geppert, C. Gorges, M. Hammen, V. Hannen, S. Kaufmann, K. König, Y. A. Litvinov,

M. Lochmann, B. Maaß, J. Meisner, T. Murböck, R. Sánchez, M. Schmidt, S. Schmidt, M. Steck, Th. Stöhlker, R. C. Thompson, C. Trageser, J. Vollbrecht, J. Weinheimer, and W. Nörthershäuser. High precision hyperfine measurements in Bismuth challenge bound-state strong-field QED. *Nat. Commun.*, 8:15484, 2017.

Acknowledgements

First of all I would like to thank my supervisor Priv. Doz. Dr. Zoltán Harman. He guided me through the whole process of the Bachelor thesis and always took his time to discuss topics and to answer questions in a very kind manner. Due to the discussions in the course of this thesis, a lecture of his I attended and his encouragement to participate in the DPG spring meeting 2018 in Erlangen, I acquired much knowledge.

I want to thank Halil Cakir for mentoring me, always being available for arising questions and sharing his knowledge with me.

I want to thank Priv. Doz. Dr. Antonino Di Piazza for evaluating this thesis.

I want to thank Dr. Natalia Oreshkina for proof reading this thesis.

I want to thank the people of the Max Planck Institute for Nuclear Physics and especially the Theory Division from Honorarprofessor Dr. Christoph H. Keitel for the hospitality during my work on the Bachelor thesis, I felt very welcome.

Erklärung

Ich versichere, dass ich diese Arbeit selbstständig verfasst und keine anderen als die angegebenen Quellen und Hilfsmittel benutzt habe.

Heidelberg, den